Engineering Letters, 18:1, EL_18_1_01

Finite Element Analysis of Magnetic Field Distribution for 500-kV Power Transmission Systems

P. Pao-la-or, A. Isaramongkolrak, and T. Kulworawanichpong

Abstract—**This paper proposes a set of mathematical models presenting magnetic fields caused by operations of an extra high voltage (EHV) transmission line under normal loading and short-circuit conditions. The mathematical models are expressed in second-order partial differential equations derived by analyzing magnetic field distribution around a 500-kV power transmission line. Finite element methods (FEM) for solving wave equations have been exploited. The modification for complex magnetic field analysis and time-harmonic simulation are also utilized. The computer simulation based on the use of the FEM has been developed in MATLAB programming environment. The problem of study is intentionally two-dimensional due to the property of long line field distribution. To verify its use, i) single-circuit and ii) double-circuit, 500-kV power transmission lines have been employed for test. From all test cases, the calculation line of 1.0 m above the ground level is set to investigate the magnetic fields acting on a human in comparative with ICNIRP standard. Moreover, visualization of magnetic fields caused by fault currents flowing through EHV transmission lines is included.**

Index Terms—**Magnetic Field, Finite Element Method (FEM), Transmission Line, Short-Circuit Faults, Computer Simulation**

I. INTRODUCTION

500-kV extra high-voltage (EHV) transmission lines of Electricity Generating Authority of Thailand (EGAT) have been increasingly installed due to electrical demand growth in Thailand. The first 500-kV power lines is a double-circuit configuration linked between Maemoh Power Plant, Lumpang province and Thatako Substation, Nakhon Sawan province. Another 500-kV power link is a single-circuit power transmission line connecting between Thatako Substation and Nongchok Substation, Bangkok. The impact of electric fields surrounding the transmission line depends strongly on conductor surface potentials, while load currents flowing through the transmission line result in magnetic field distribution. For the 500 kV systems, high current density transmission is the main purpose. It can cause electrical hazards to people or their livestock nearby. Especially when the power system was faulted, the short-circuit current is much higher than the normal current loading. This paper focuses on utilization of efficient computing techniques to estimate the magnetic field distribution. Obtained estimate solutions can lead to assessment of electrical hazards for 500-kV power transmission systems.

Finite Element Method (FEM) is one among popular numerical methods that is able to handle problem complexity in various forms. At present, the FEM has been widely applied in most engineering fields. Even for problems of magnetic field distribution, the FEM is able to estimate solutions of Maxwell's equations governing the 500-kV power transmission systems. Potential and electric field analysis resulting from high voltage conductor potentials of a power transmission lines have been increasingly reported. In contrast, most of magnetic field analyses in high voltage power transmission systems focus on magnetic shielding problems [1]-[3]. There are some works studying effects of magnetic fields on environment surrounding a power line carrying high current. By literature, these research works are conducted based on electromagnetic theory or image theory [4], [5]. With defining a line of calculation and assuming very thin power lines, two-dimensional problems of magnetic field analysis governed by empirical mathematical expressions can be applied. However, these conventional methods are unable to include effects of bundled conductors that are typical for EHV power transmission systems. To provide a potential tool of simulation, the FEM is flexible and suitable to estimate magnetic field distribution. Although the conventional methods are simpler than the use of the FEM, they are limited for the system of simple geometry. In practice, several metallic structures can be found underneath the power transmission line, e.g. steel tower trusts, communication lines nearby, metallic fends or other lower voltage transmission lines. Employing the FEM can includes these effects by choosing material magnetic permeability for each additional structure domain. With this feature, the FEM is one of potential numerical simulation tools for analyzing magnetic field problems of combined material regions. Unfortunately, there is no report of exploiting the FEM for magnetic field analysis of electric power transmission systems. To utilize the advantages of the FEM for handling the magnetic field problems, FEM model development and problem formulation need to be defined in magnetic field problems of EHV power transmission systems.

P. Pao-la-or is with the School of Electrical Engineering, Institute of Engineering, Suranaree University of Technology, Nakhon Ratchasima, THAILAND (corresponding author to provide phone: 0-4422-4400; fax: 0-4422-4601; e-mail: padej@sut.ac.th).

A. Isaramongkolrak is with the School of Electrical Engineering, Institute of Engineering, Suranaree University of Technology, Nakhon Ratchasima, THAILAND (e-mail: anone_91@hotmail.com).

T. Kulworawanichpong is with the School of Electrical Engineering, Institute of Engineering, Suranaree University of Technology, Nakhon Ratchasima, THAILAND (e-mail: thanatchai@gmail.com).

(Advance online publication: 1 February 2010)

In this paper, magnetic field modelling of power transmission lines is briefed in Section II. Section III is to illustrate the utilization of the FEM for the magnetic field modelling described in Section II. Section IV gives simulation results in both normal and faulted conditions, and discussion. Test cases given in this paper is the 500-kV transmission line that has been installed in Thailand. It is currently the highest operating voltage level in this country. The simulation conducted herein is based on the FEM method given in Section III. All the programming instructions are coded in MATLAB program environment. Moreover, due to excessive magnetic fields that might be harmful to people or livestock living nearby, careful investigation of the magnetic phenomena is taken into account. According to the standard of International Commission of Non Ionizing Radiation Protection (ICNIRP), the satisfactory simulation results are also complied with the ICNIRP standard.

II. MAGNETIC FIELD MODELING FOR A POWER TRANSMISSION LINE

The mathematical model representing magnetic fields (**B**) caused by a power transmission line carrying high current is expressed in form of the magnetic field intensity (**H**) in which $\mathbf{B} = \mu\mathbf{H}$. Utilizing the wave equation (Helmholtz's equation) as in (1) [6], [7], magnetic field modeling that follows the Ampere's circuital law is defined.

$$\nabla^2\mathbf{H} - \sigma\mu\frac{\partial\mathbf{H}}{\partial t} - \varepsilon\mu\frac{\partial^2\mathbf{H}}{\partial t^2} = 0 \tag{1}$$

where ε is the constant dielectric permittivity, μ is the magnetic permeability, and σ is the conductivity.

This paper has considered the time-harmonic system by representing $\mathbf{H} = He^{j\omega t}$ [8], therefore

$$\frac{\partial\mathbf{H}}{\partial t} = j\omega H \quad \text{and} \quad \frac{\partial^2\mathbf{H}}{\partial t^2} = -\omega^2 H$$

where ω is the angular frequency

Therefore, refer to (1) can be rewritten into the following equation.

$$\nabla^2 H - j\omega\sigma\mu H + \omega^2\varepsilon\mu H = 0$$

Considering the problem in two dimensional *(x,y)* plane, then

$$\frac{\partial}{\partial x}\left(\frac{1}{\mu}\frac{\partial H}{\partial x}\right) + \frac{\partial}{\partial y}\left(\frac{1}{\mu}\frac{\partial H}{\partial y}\right) - \left(j\omega\sigma - \omega^2\varepsilon\right)H = 0 \tag{2}$$

As can be seen, to obtain an exact solution of (2) is difficult. In this paper, the FEM has been employed to find an approximate solution [9].

III. FEM FOR THE POWER TRANSMISSION LINE

A. *Discretization*

This research is to focus on a power transmission system of Electric Generating Authority of Thailand (EGAT), especially single- and double-circuit, 500-kV power transmission line. Both circuits are 4-bundled conductors as illustrated diagrammatically by Fig. 1 and Fig. 2, respectively. The height of the lowest conductors at midspan (maximum sag allowance) for both circuit types is 13.00 m above the ground level [10]. Phase conductors used are 795 MCM (diameter = 0.02772 m) while overhead ground wires (OHG) are 3/8 inch (diameter = 0.009114 m).

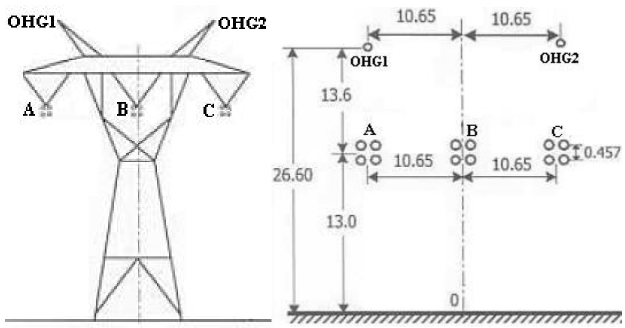

Fig. 1 Single circuit 500 kV transmission system with dimension (m)

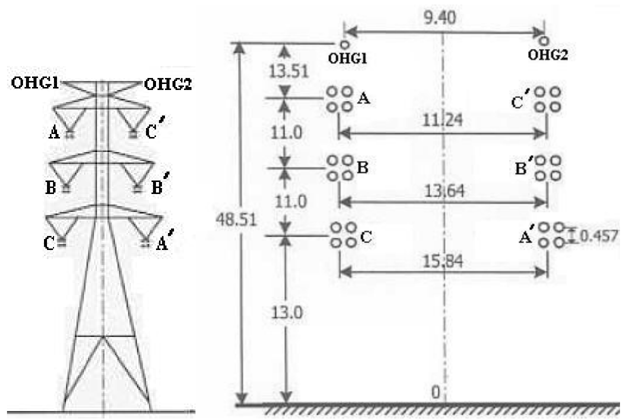

Fig. 2 Double circuit 500 kV transmission system with dimension (m)

The working region for modelling magnetic fields using FEM is defined by Fig. 3 and Fig. 4, which are decretized by using linear triangular elements.

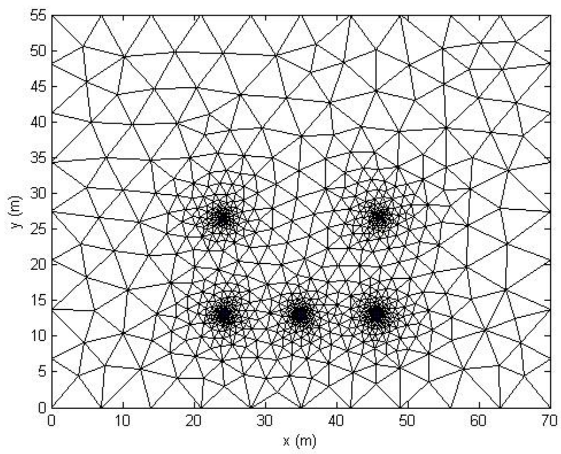

Fig. 3 Discretization of a single circuit transmission system

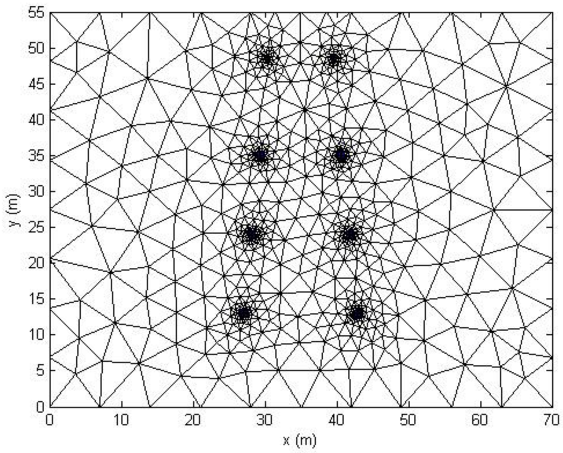

Fig. 4 Discretization of a double circuit transmission system

B. *Finite Element Formulation*

An equation governing each element is derived from the Maxwell's equations directly by using Galerkin approach, which is the particular weighted residual method for which the weighting functions are the same as the shape functions [11], [12]. According to the method, the electric field is expressed as

$$H(x,y) = H_i N_i + H_j N_j + H_k N_k \tag{3}$$

where N_n , $n = i, j ,k$ is the element shape function and the H_n , $n = i, j ,k$ is the approximation of the magnetic field intensity at each node (i, j ,k) of the elements, which is

$$N_n = \frac{a_n + b_n x + c_n y}{2\Delta_e}$$

where Δ_e is the area of the triangular element and,

$$\begin{aligned} a_i &= x_j y_k - x_k y_j, & b_i &= y_j - y_k, & c_i &= x_k - x_j \\ a_j &= x_k y_i - x_i y_k, & b_j &= y_k - y_i, & c_j &= x_i - x_k \\ a_k &= x_i y_j - x_j y_i, & b_k &= y_i - y_j, & c_k &= x_j - x_i. \end{aligned}$$

The method of the weighted residual with Galerkin approach is then applied to the differential equation, refer to (2), where the integrations are performed over the element domain Ω.

$$\int_\Omega N_n \left(\frac{\partial}{\partial x}\left(\frac{1}{\mu}\frac{\partial H}{\partial x}\right) + \frac{\partial}{\partial y}\left(\frac{1}{\mu}\frac{\partial H}{\partial y}\right)\right) d\Omega - \int_\Omega N_n \left(j\omega\sigma - \omega^2\varepsilon\right) H \, d\Omega = 0$$

,or in the compact matrix form

$$\left[M + K\right]\left\{H\right\} = 0 \tag{4}$$

$$M = \left(j\omega\sigma - \omega^2\varepsilon\right)\int_\Omega N_n N_m d\Omega = \frac{\left(j\omega\sigma - \omega^2\varepsilon\right)\Delta_e}{12}\begin{bmatrix} 2 & 1 & 1 \\ 1 & 2 & 1 \\ 1 & 1 & 2 \end{bmatrix}$$

$$K = \frac{1}{\mu}\int_\Omega \left(\frac{\partial N_n}{\partial x}\frac{\partial N_m}{\partial x} + \frac{\partial N_n}{\partial y}\frac{\partial N_m}{\partial y}\right) d\Omega = \frac{1}{4\mu\Delta_e}\begin{bmatrix} b_i b_i + c_i c_i & b_i b_j + c_i c_j & b_i b_k + c_i c_k \\ b_i b_j + c_i c_j & b_j b_j + c_j c_j & b_j b_k + c_j c_k \\ b_i b_k + c_i c_k & b_j b_k + c_j c_k & b_k b_k + c_k c_k \end{bmatrix}$$

For one element containing 3 nodes, the expression of the FEM approximation is a 3×3 matrix. With the account of all elements in the system of n nodes, the system equation is sizable as an $n \times n$ matrix.

C. *Boundary Conditions and Simulation Parameters*

The boundary conditions applied here are zero magnetic fields at the ground and the OHG. For the boundary conditions at outer perimeters of 12-single circuit power lines and 24-double circuit power lines has applied with the research of [10], [13], which boundary conditions of magnetic field depends on the load current. Both single and double circuits are considered by the maximum load current of 3.15 kA per phase [10] and assumed to be a balanced load condition. For faulted conditions [14], the single line-to-ground faults is assumed that phase A is shorted to ground so that $I_A = 4.95\angle{-90°}$ p.u., $I_B = I_C = 0$. The double line-to-ground faults between phase B and C caused the fault currents of $I_A = 0$, $I_B = 3.36\angle 151.77°$ p.u., $I_C = 3.36\angle 28.23°$ p.u. For the line-to-line faults of phase B and C, $I_A = 0$, $I_B = -I_C = 3.34\angle{-180°}$ p.u. The last fault case is the balanced three-phase faults in which $I_A = 3.23\angle{-90°}$ p.u., $I_B = 3.23\angle{-210°}$ p.u., $I_C = 3.23\angle 30°$ p.u. The conductors used for test are Aluminum Conductor Steel Reinforced (ACSR) having the following properties: conductivity (σ) = 0.8×10^7 S/m, the relative permeability (μ_r) = 300, and the relative permittivity (ε_r) = 3.5. It notes that the permittivity of free space (ε_0) = 8.854×10^{-12} F/m and the permeability of free space (μ_0) = 4π×10^{-7} H/m [15].

IV. RESULT AND DISCUSSION

A. Normal Loading

The FEM-based simulation conducted in this paper is coded with MATLAB programming for calculation of magnetic field dispersion. To utilize a graphical feature of MATLAB, the contour of magnetic field distribution through the cross-sectional area of the working domain for the single- and double-circuit transmission systems are presented in Fig. 5 and Fig. 6, respectively.

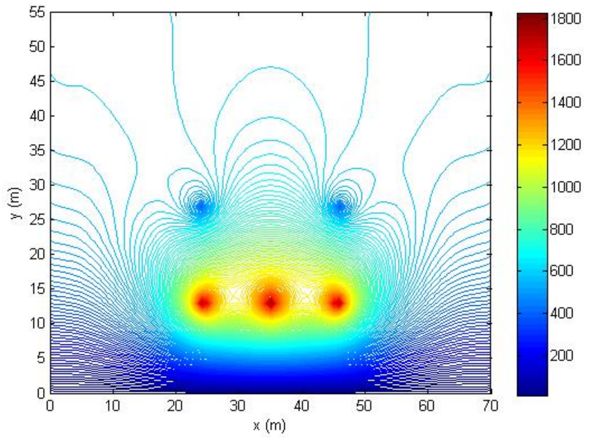

Fig. 5 Magnetic field distribution (μT) for the single-circuit case

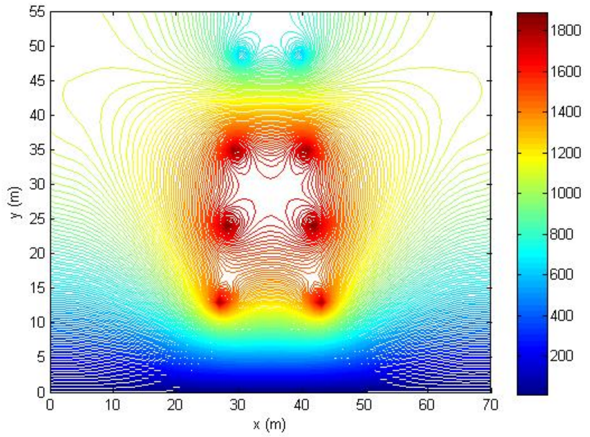

Fig. 6 Magnetic field distribution (μT) for the double-circuit case

The illustration of magnetic field contour for both single- and double-circuit systems is given by a working area of the 70×55 m^2 rectangle as shown in Fig. 3 and Fig. 4, respectively. The magnetic field distributions simulated are determined by balanced carrying currents in the phase conductors. Magnetic field distribution of the double-circuit case is higher than that of the single-circuit case. To describe possible effects of magnetic field strength on human or other living things underneath the power line, the line of calculation, 1.0 m above the ground (y = 1 m) is defined. The comparative result of magnetic field for both single- and double-circuit cases is shown in Fig. 7. It notices that each graph has two peaks near the center position.

Table I showed the result of comparison in magnetic field distribution through distance x when consider single and double circuit transmission line that is over from the ground level 1 m that people pass by. An average of magnetic field through distance x of single and double circuit when consider the height of transmission line at midspan and consider at maximum load current are 65.88 μT and 74.18 μT, respectively, which is less than magnetic field level that hazard to human. It is regulated by International Commission of Non Ionizing Radiation Protection [16], which the level of magnetic field safe to human for general public up to 24 hours/day must not greater than 100 μT and for occupation whole working day must not over 500 μT. Fig. 8 - Fig .18 are graphs representing the magnetic fields of both single and double circuit cases at a position of 5, 10, 15, 20, 25, 30, 35, 40, 45, 50 and 55 m above ground level, respectively. Table II showed comparative results among average magnetic field for all the cases. It is considered that at the same height, the double circuit distributes more intensive magnetic field than the single circuit does due to twice of the conductor number.

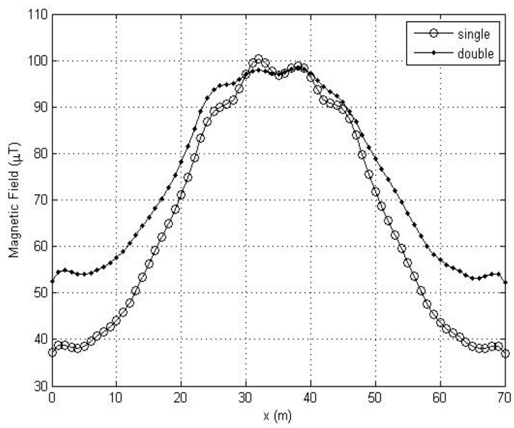

Fig. 7 Magnetic field (T) at high 1 m

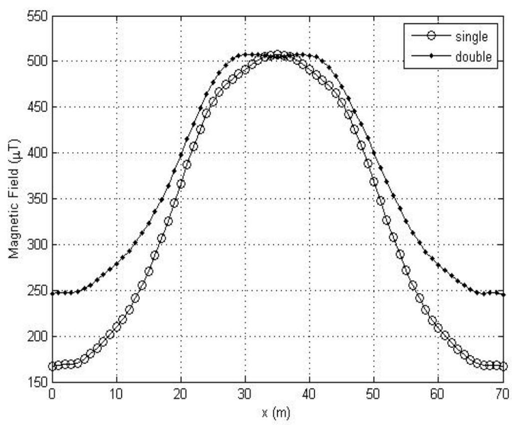

Fig. 8 Magnetic field (T) at high 5 m

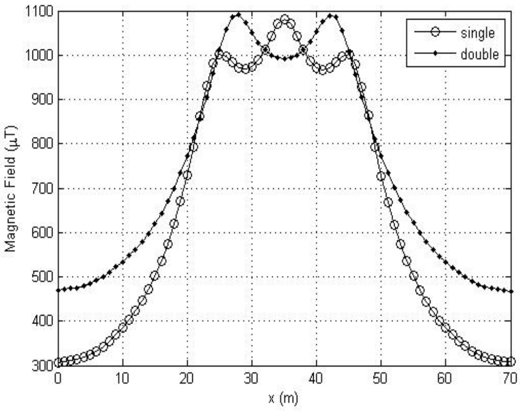

Fig. 9 Magnetic field (T) at high 10 m

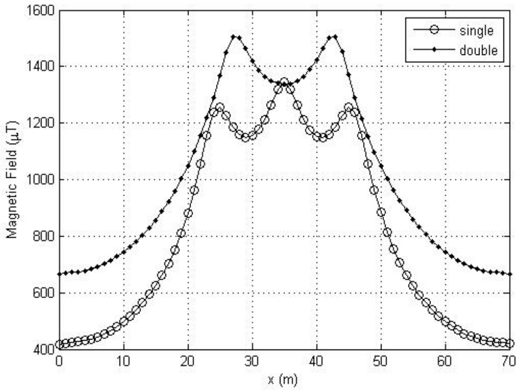

Fig. 10 Magnetic field (T) at high 15 m

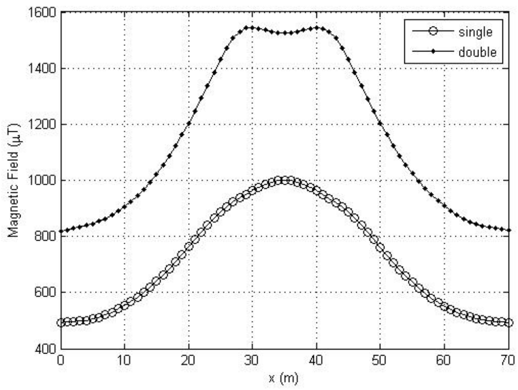

Fig. 11 Magnetic field (T) at high 20 m

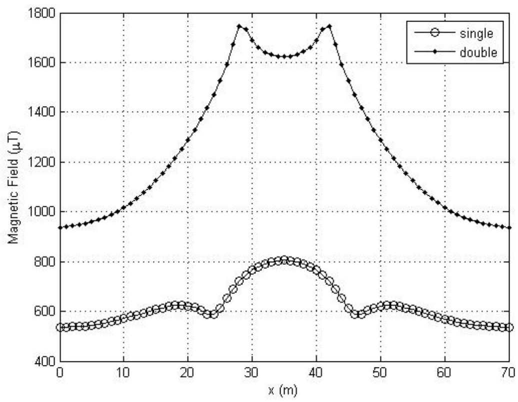

Fig. 12 Magnetic field (T) at high 25 m

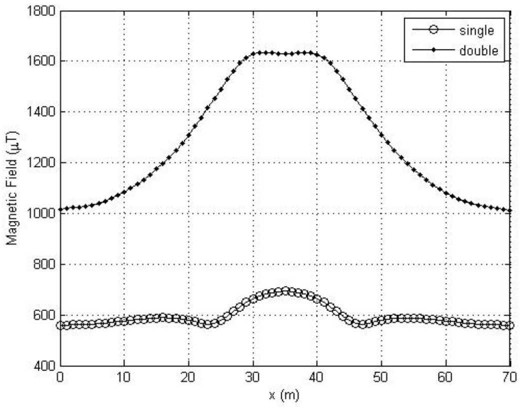

Fig. 13 Magnetic field (T) at high 30 m

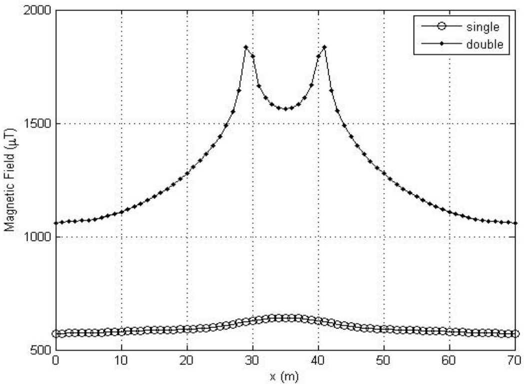

Fig. 14 Magnetic field (T) at high 35 m

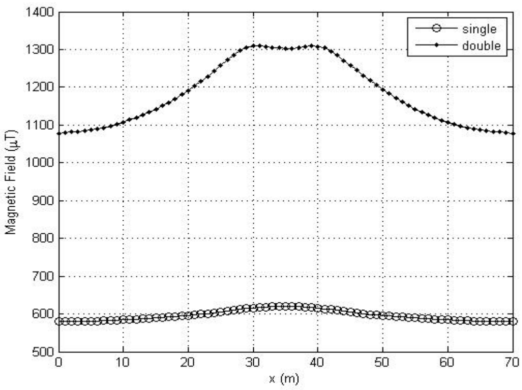

Fig. 15 Magnetic field (T) at high 40 m

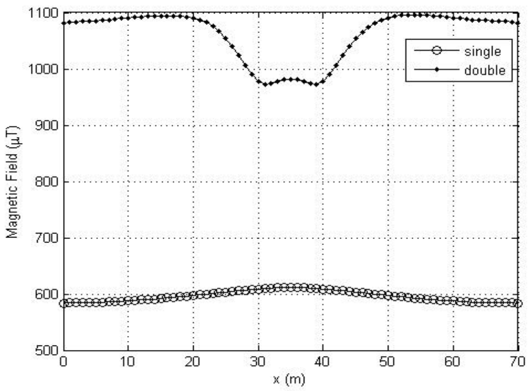

Fig. 16 Magnetic field (T) at high 45 m

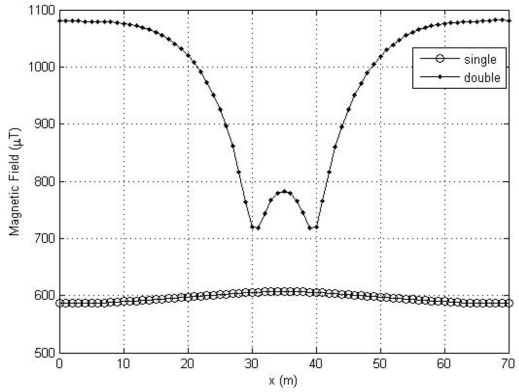

Fig. 17 Magnetic field (T) at high 50 m

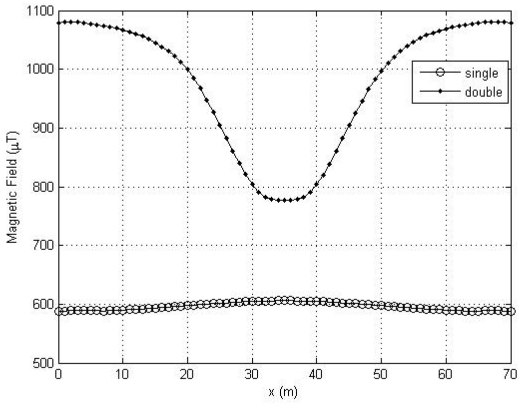

Fig. 18 Magnetic field (T) at high 55 m

B. Fault Conditions

The contour of magnetic field distribution through the cross-sectional area of the working domain for the single-circuit transmission systems for four faulted conditions (single line-to-ground faults, double line-to-ground faults, line-to-line faults and balanced three-phase faults) are presented in Fig. 19 - Fig. 22, respectively. The double-circuit transmission systems for the four faulted cases are presented in Fig. 23 - Fig. 26, respectively.

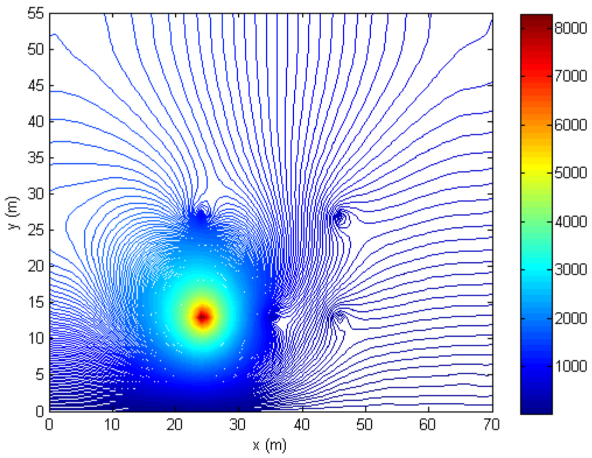

Fig. 19 Magnetic field distribution (μT) for the single-circuit case of the single line-to-ground faults

Table I
Comparing of magnetic field dispersion at high 1 m

x (m)	Single (μT)	Double (μT)	*x* (m)	Single (μT)	Double (μT)
1	37.11	52.54	36	97.17	97.41
2	38.67	54.57	37	98.28	98.04
3	38.74	54.84	38	98.87	98.36
4	38.34	54.42	39	98.28	98.10
5	38.18	54.00	40	96.38	97.20
6	38.60	53.96	41	93.77	95.79
7	39.56	54.34	42	91.59	94.35
8	40.72	54.98	43	90.74	93.35
9	41.74	55.69	44	90.40	92.39
10	42.77	56.52	45	89.49	91.02
11	44.06	57.59	46	87.40	89.13
12	45.76	58.94	47	84.04	86.75
13	47.95	60.60	48	79.83	84.04
14	50.60	62.52	49	75.54	81.33
15	53.46	64.49	50	71.87	78.94
16	56.25	66.34	51	68.64	76.71
17	59.04	68.23	52	65.57	74.44
18	61.92	70.33	53	62.54	72.07
19	64.88	72.69	54	59.54	69.63
20	67.91	75.33	55	56.58	67.17
21	71.14	78.25	56	53.59	64.72
22	74.83	81.59	57	50.54	62.29
23	79.13	85.38	58	47.72	60.11
24	83.39	89.00	59	45.41	58.36
25	86.83	91.85	60	43.66	57.04
26	89.02	93.68	61	42.39	56.10
27	90.05	94.54	62	41.44	55.37
28	90.52	94.75	63	40.51	54.64
29	91.50	94.99	64	39.40	53.81
30	93.94	95.91	65	38.46	53.18
31	96.97	97.02	66	38.03	53.07
32	99.43	97.78	67	38.18	53.51
33	100.33	98.00	68	38.57	54.12
34	99.47	97.74	69	38.54	54.11
35	97.81	97.24	70	37.03	52.37
			Average	**65.88**	**74.18**

Table II
Comparing of average of magnetic field at each height

y (m)	Single (μT)	Double (μT)	*y* (m)	Single (μT)	Double (μT)
1	66	74	30	596	1288
5	327	371	35	596	1299
10	652	740	40	596	1182
15	810	1016	45	596	1061
20	719	1157	50	596	978
25	627	1269	55	596	977

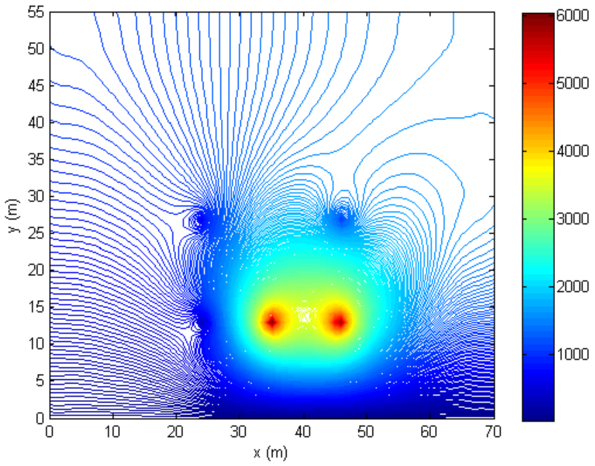

Fig. 20 Magnetic field distribution (μT) for the single-circuit case of the double line-to-ground faults

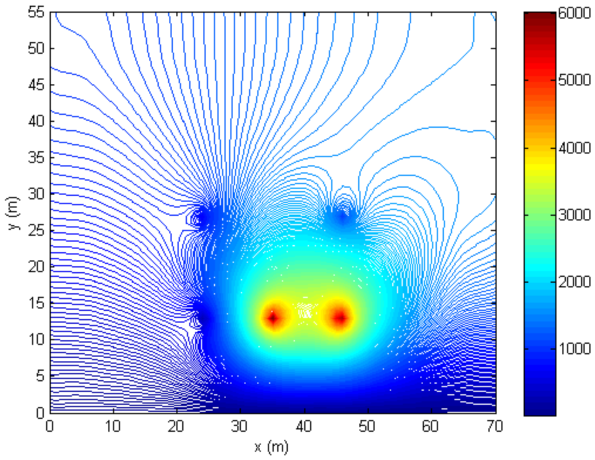

Fig. 21 Magnetic field distribution (μT) for the single-circuit case of the line-to-line faults

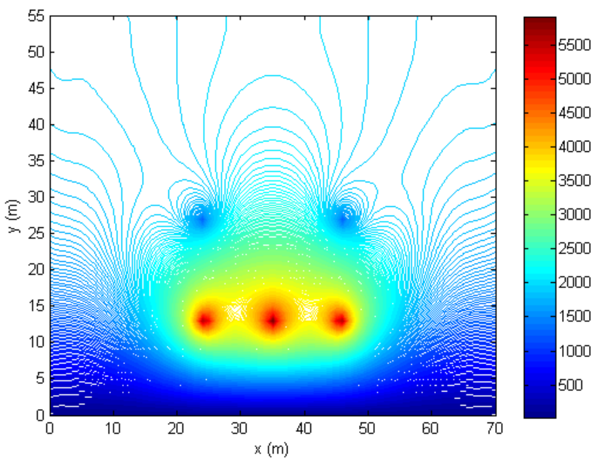

Fig. 22 Magnetic field distribution (μT) for the single-circuit case of the balanced three-phase faults

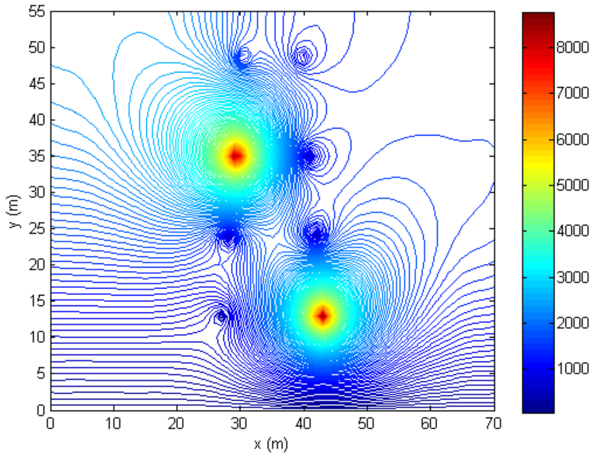

Fig. 23 Magnetic field distribution (μT) for the double-circuit case of the single line-to-ground faults

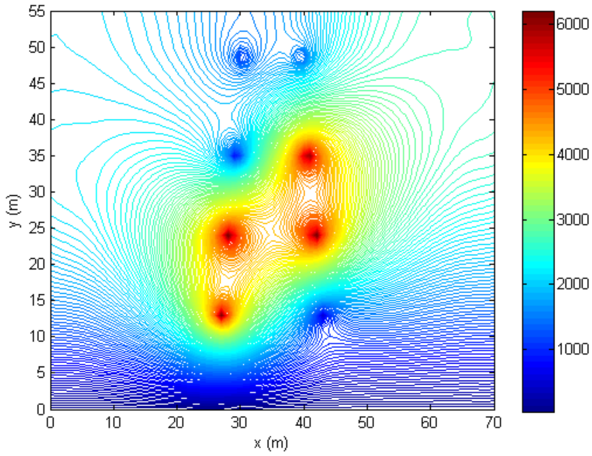

Fig. 24 Magnetic field distribution (μT) for the double-circuit case of the double line-to-ground faults

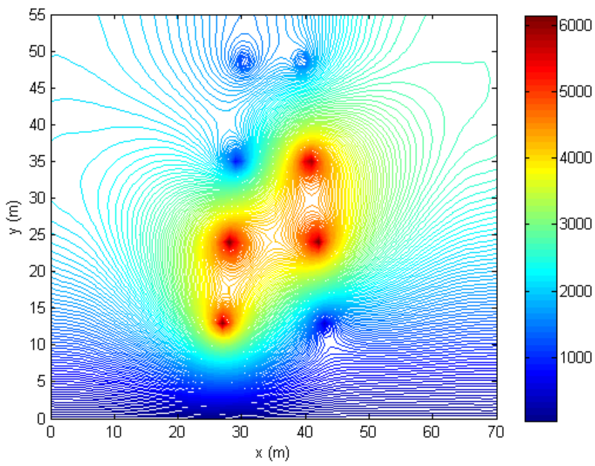

Fig. 25 Magnetic field distribution (μT) for the double-circuit case of the line-to-line faults

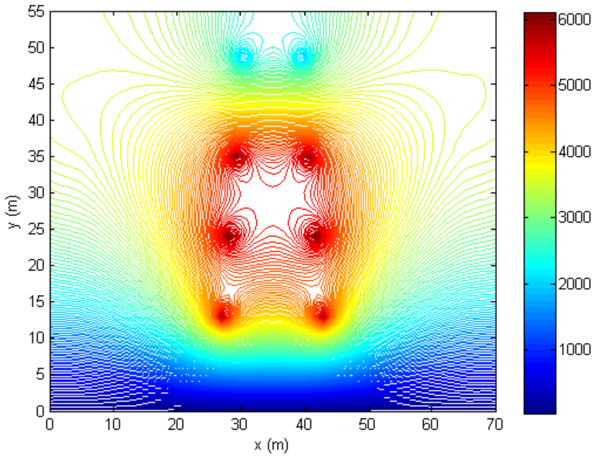

Fig. 26 Magnetic field distribution (μT) for the double-circuit case of the balanced three-phase faults

From Fig. 19 - Fig. 26, magnetic field contour of the faulted cases for both single- and double-circuit systems are presented. Table III – VI show the average of magnetic fields for both single- and double-circuit systems at each height when the single line-to-ground faults, double line-to-ground faults, line-to-line faults and balanced three-phase faults are occurred, respectively. As can be seen, the magnetic field intensity caused by the faulted cases is remarkably higher than that of the normal conditions. However, due to the reliable operation of protective devices in electric power systems this could not harm human or other living things underneath the EHV power lines.

Table III
Average of magnetic field at each height of the single line-to-ground faults

y (m)	Single (μT)	Double (μT)	y (m)	Single (μT)	Double (μT)
1	119	142	30	1091	2086
5	591	715	35	1091	2463
10	1177	1424	40	1091	2241
15	1462	1801	45	1091	2001
20	1307	1699	50	1091	1835
25	1145	1691	55	1091	1834

Table IV
Average of magnetic field at each height of the double line-to-ground faults

y (m)	Single (μT)	Double (μT)	y (m)	Single (μT)	Double (μT)
1	147	160	30	1334	3036
5	727	799	35	1333	2828
10	1450	1593	40	1334	2575
15	1802	2289	45	1334	2319
20	1603	2842	50	1334	2141
25	1402	3233	55	1335	2139

Table V
Average of magnetic field at each height of the line-to-line faults

y (m)	Single (μT)	Double (μT)	y (m)	Single (μT)	Double (μT)
1	145	158	30	1319	3010
5	719	790	35	1318	2801
10	1434	1574	40	1319	2550
15	1782	2265	45	1319	2296
20	1584	2816	50	1319	2120
25	1386	3206	55	1319	2118

Table VI
Average of magnetic field at each height of the balanced three-phase faults

y (m)	Single (μT)	Double (μT)	y (m)	Single (μT)	Double (μT)
1	213	240	30	1949	4159
5	1060	1199	35	1948	4196
10	2113	2390	40	1949	3819
15	2626	3282	45	1949	3428
20	2339	3736	50	1949	3158
25	2047	4098	55	1950	3155

V. Conclusion

This paper has studied the magnetic field distribution surrounding EHV transmission line in both normal loadings and faulted conditions in which the single line-to-ground faults, double line-to-ground faults, line-to-line faults and balanced three-phase faults were situated. Single- and double-circuit, 500-kV transmission lines of Electricity Generating Authority of Thailand (EGAT), which is recently the highest voltage level in Thailand, are investigated. The computer simulation is performed by using finite element methods instructed in MATLAB programming codes. The results of the normal loading case revealed that the magnetic fields from both single- and double-circuit, 500-kV transmission lines at a level of 1 m above the ground that are assumed to be the level of human working, do not excess the maximum allowance when compiled with the ICNIRP standard. Additionally, the results also showed that the magnetic intensity of the double circuit cases is normally stronger than those of the single circuits.

References

[1] Y. Du, T.C. Cheng and A.S. Farag, "Principles of Power-Frequency Magnetic Field Shielding with Flat Sheets in a Source of Long Conductors," *IEEE Transactions on Electromagnetic Compatibility*, Vol. 38, No. 3, pp.450-459, 1996.

[2] A.R. Memari and W. Janischewskyj, "Mitigation of Magnetic Field near Power Lines," *IEEE Transactions on Power Delivery*, Vol. 11, No. 3, pp.1577-1586, 1996.

[3] K. Wassef, V.V. Varadan and V.K. Varadan, "Magnetic Field Shielding Concepts for Power Transmission Lines," *IEEE Transactions on Magnetics*, Vol. 34, No. 3, pp.649-654, 1998.

[4] R.G. Olsen, D. Deno, R.S. Baishiki, J.R. Abbot, R. Conti, M. Frazier, K. Jaffa, G.B. Niles, J.R. Stewart, R. Wong and R.M. Zavadil, "Magnetic Fields from Electric Power Lines Theory and Comparison to Measurements," *IEEE Transactions on Power Delivery*, Vol. 3, No. 4, pp.2127-2136, 1988.

[5] L. Li and G. Yougang, “Analysis of Magnetic Field Environment near High Voltage Transmission Lines,” *Proceedings of the International Conferences on Communication Technology*, pp.S26-05-1 - S26-05-5, 1998.

[6] M.V.K. Chari and S.J. Salon, *Numerical Methods in Electromagnetism*, Academic Press, USA, 2000.

[7] M. Weiner, *Electromagnetic Analysis Using Transmission Line Variables*, World Scientific Publishing, Singapore, 2001.

[8] C. Christopoulos, *The Transmission-Line Modeling Method: TLM*, IEEE Press, USA, 1995.

[9] P. Pao-la-or, T. Kulworawanichpong, S. Sujitjorn and S. Peaiyoung, “Distributions of Flux and Electromagnetic Force in Induction Motors: A Finite Element Approach,” *WSEAS Transactions on Systems*, Vol. 5, No. 3, pp.617-624, 2006.

[10] P. Pin-anong, *The Electromagnetic Field Effects Analysis which Interfere to Environment near the Overhead Transmission Lines and Case Study of Effects Reduction*, M. Eng. Thesis, King Mongkut’s Institute of Technology Ladkrabang, Bangkok, Thailand, 2002.

[11] T.W. Preston, A.B.J. Reece and P.S. Sangha, “Induction Motor Analysis by Time-Stepping Techniques,” *IEEE Transactions on Magnetics*, Vol. 24, No. 1, pp.471-474, 1988.

[12] B.T. Kim, B.I. Kwon and S.C. Park, “Reduction of Electromagnetic Force Harmonics in Asynchronous Traction Motor by Adapting the Rotor Slot Number,” *IEEE Transactions on Magnetics*, Vol. 35, No. 5, pp.3742-3744, 1999.

[13] G.B. Iyyuni and S.A. Sebo, “Study of Transmission Line Magnetic Fields,” *Proceedings of the Twenty-Second Annual North American, IEEE Power Symposium*, pp.222-231, 1990.

[14] M.E. El-Hawary, *Electrical Energy Systems*, CRC Press, USA, 2000.

[15] Jr.W.H. Hayt and J.A. Buck, *Engineering Electromagnetics (7th edition)*, McGraw-Hill, Singapore, 2006.

[16] International Commission of Non Ionizing Radiation Protection (ICNIRP), “Guidelines for Limiting Exposure to Time-Varying Electric, Magnetic and Electromagnetic Fields (up to 300 GHz),” *Health Phys.*, Vol. 74, No. 4, pp.494-522, 1998.